Supporting Information

Dual roles of graphitic carbon nitride in the electrosynthesis of ammonia under ambient conditions

Lu Liu, Luofu Min, Wen Zhang, Yuxin Wang**

State Key Laboratory of Chemical Engineering, Tianjin Key Laboratory of Membrane Science & Desalination Technology, and School of Chemical Engineering and Technology, Tianjin University, Tianjin, 300350, China

*Corresponding authors

E-mail addresses: zhang_wen@tju.edu.cn (W Zhang)

yxwang@tju.edu.cn (Y Wang)

Experimental section

Membrane pretreatment

Before NRR tests, the Nafion 212 membrane was pretreated by heating it in H_2O_2 (3 wt%) aqueous solution at 80 °C for 1h, ultrapure water at 80 °C for 1h and 0.5 mol/L H_2SO_4 aqueous solutions for another 1h, respectively.

Preparation of the Gas diffusion layer (GDL)

Cathode preparation: Typically, approximately 3 mg catalyst and 20 μL of Nafion solution (5 wt%) were dispersed into a mixture of H_2O:IPA (50:50) by sonicating for 1 h to form a homogeneous ink and hand-sprayed onto a carbon paper electrode with the area of 1.1×3.6 cm^2 and dried under the ambient condition to serve as the cathode.

Anode preparation: The ink solution of Pt/C was prepared following the same procedure outline above and was subsequently sprayed onto a carbon paper with the Pt loading of 0.2 mg/cm^2, which was used as the anode.

Membrane electrode assembly (MEA)

The GDL after spraying the catalyst and on the pretreated Nafion 212 membrane were hot-pressed together at 10 MPa and 120 ^oC for 120 s. The active composite material was located between these two layers. The MEA was fabricated for electrochemical nitrogen reduction reaction with an active geometric cross-sectional area of 3.96 cm^2 (Figure S1).

Detection of ammonia

The amount of ammonia in the effluent of cathode and anode, as well as in the soaking solution of the used MEA, was determined using the indophenol blue method with some modification[1]. In detail, a certain volume cathodic absorption solution removed from the vessel, and subsequently added into 0.5 mL of 50 g/L (5 wt%) salicylic acid solution

containing sodium citrate and sodium hydroxide. And Then, 0.1 mL of 10 g/L (1 wt %) $C_5FeN_6Na_2O$ (sodium nitroferricyanide) and 0.1 mL of 0.05 mol/L NaClO containing 2 mol/L NaOH were also added into the above solution. After standing at room temperature for 1 hour, the UV-Vis absorption spectrum was measured. The absorbance data of the spectrophotometer were measured on the Beijing Purkinje General TU-1900 ultraviolet-visible (UV-Vis) spectrophotometer. The concentration of indophenol blue was determined using the absorbance at a wavelength of 697 nm. The concentration-absorbance curves were calibrated using a standard ammonia chloride solution with a series of concentrations. The fitting curve ($y = 0.8775x + 0.0358$, $R^2 = 0.9998$) shows good linear relation of absorbance value with ammonia concentration by four times independent calibrations (Figure S5).

Detection of hydrazine

The hydrazine in the effluent of cathode and anode, as well as in the soaking solution of the used MEA, was estimated by the method of Watt and Chrisp[2]. A mixture of p-dimethylaminobenzaldehyde (*p*-$C_9H_{11}NO$, 5.99 g), HCl (concentrated, 30 mL), and C_2H_5OH (300 mL) was used as a color reagent. The calibration curve was plotted as follows. A series of 5 mL standard N_2H_4 solutions with the concentrations of 0.0, 0.05, 0.1, 0.2, 0.3, 0.4, 0.6, 0.8 and 1.0 μg/mL in 0.005 mol/L H_2SO_4 solution were prepared, and separately mixed with 5 mL above prepared color reagent. After stirring the mixed solution for 10 min at room temperature, the absorbance of the resulting solution was measured at 455 nm, and the yields of N_2H_4 were estimated from a standard curve (Figure S6. In this study, the byproduct of N_2H_4 is not detected, implying the good selectivity of the as-synthesized catalyst.

Faradaic efficiency（FE）

The Faradaic efficiency for ENRR was defined as the quantity of electric charge used for synthesizing ammonia divided by the total charge pass through the electrodes during the

electrolysis. The total amount of ammonia produced was measured using indophenol blue colorimetric methods. Assuming three electrodes were needed to produce one NH_3 molecule, the Faradaic efficiency can be calculated as follows:

$$\mathrm{FE}(\%)=\frac{3\times n\times F}{I(A)\times t(s)}\times 100\%$$

Where: F is Faraday constant, I(A) is the average of current during the reaction.

N-15 labeling experiments

Labeled ^{15}N isotopic labeling g-$C_3{}^{15}N_4$ was used as the catalyst to prove that the N atom in the catalyst is involved in the formation of ammonia, subsequently, the N vacancy is created, and then the N vacancy could adsorb and activate N_2. We used g-$C_3{}^{15}N_4$ as the catalyst, feeding by Ar or N_2 in the cathode and H_2 in the anode, then used MEA was soaked in 0.005 M H_2SO_4 aqueous solutions to extract the $^{14}NH_4^+$ and $^{15}NH_4^+$ inside the membrane after the ENRR test.

Indophenol assays[3] were prepared from 0.5 ml of aliquots solution in the effluent of cathode and the soaking solution of the used MEA, reacted with 0.1 ml of 1% phenolic solution in 95% ethanol/water (1.2 g of phenol in 10 ml of 95% ethanol/water), 0.1mL of 0.5% $Na[Fe(CN)_5NO]$ in water and 0.375 ml of 1% NaClO in alkaline sodium citrate solution (2g of sodium citrate and 0.1g of NaOH in 10 mL of water mixed with 2.5 mL of 5% NaClO solution). The assayed aliquots were allowed to develop 1 hour before spectrophotometric testing. LC-MS studies were carried on an ACQUITY UPLC I-Class/UPCC/M-Class/SYNAPT G2-SI (LCMS–ESI). For comparison, the indophenol assay was prepared from the soaking solution of the used MEA for LC-MS detection when the unlabeled g-C_3N_4 was used as the cathode catalyst. In this study, atmosphere control experiments found that the electroreduction N_2 to NH_3 over the catalyst g-C_3N_4 may obey the MvK like mechanism.

DFT Calculation

In this study, only the tri-s-triazine-based g-C_3N_4 was invenstigated because it was energetically favored and was the most stable phase of C_3N_4 at ambient conditions.[4] All of the atoms were fully opyimized. The DFT calculations were performed using Gaussian09. [5] For geometry optimization and frequency calculations, the UB3LYP[6] functional was adopted. The 6-31G(d,p) basis set[7, 8] was used for C and N atoms in combination with the D3(BJ) empirical dispersion correction[9, 10]. The fringe C/N atoms were compensated by H to eliminate boundary influence. All structures have converged to the minimum energy point, and there is no false frequency.

Figures:

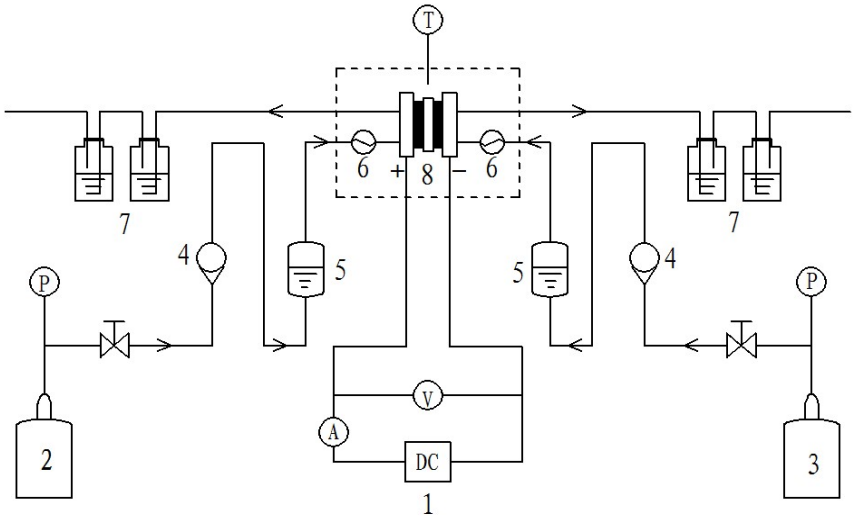

Figure S1 Flow chart of electrochemical synthesis of ammonia

1—DC regulated power supply, 2— H_2 gas cylinder, 3— N_2/Ar gas cylinder, 4— rotor flow meter, 5— bubbling humidifier, 6— preheating pipe, 7— ammonia absorber, 8— single-cell.

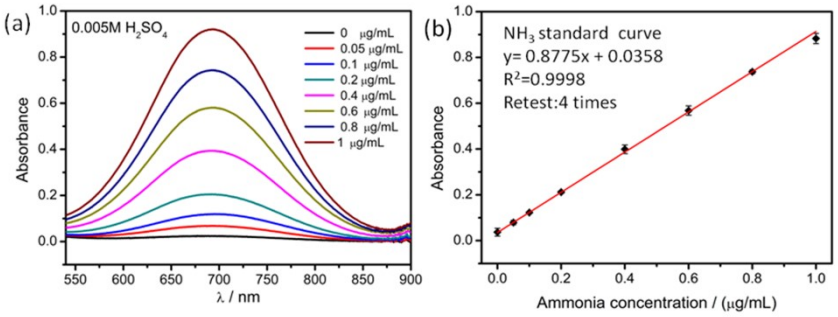

Figure S2 Absolute calibration of the indophenol blue method using ammonium chloride in 0.005 M H_2SO_4 solutions of known concentration as standards. (a) UV-vis curves of indophenol assays with NH_4^+ ions after incubated for 1 hour and (b) calibration curve used for estimation of NH_3 by NH_4^+ ion concentration. The absorbance at 697 nm was measured by UV-vis spectrophotometer, and the fitting curve shows good linear relation of absorbance with NH_4^+ ion concentration (y = 0.8775x +0.0358, R^2 = 0.9998) of four times independent calibration curves.

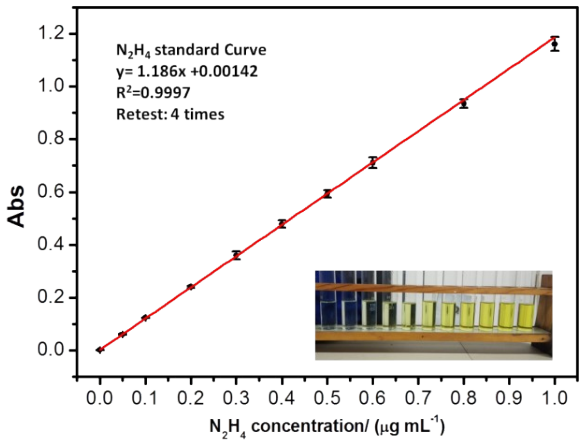

Figure S3 The calibration curve used for estimation of N_2H_4 concentration. The absorbance at 455 nm was measured by UV-vis spectrophotometer, and the fitting curve shows good linear relation of absorbance with N_2H_4 concentration (y = 1.186x +0.00142, R^2 = 0.9997) of four times independent calibration curves

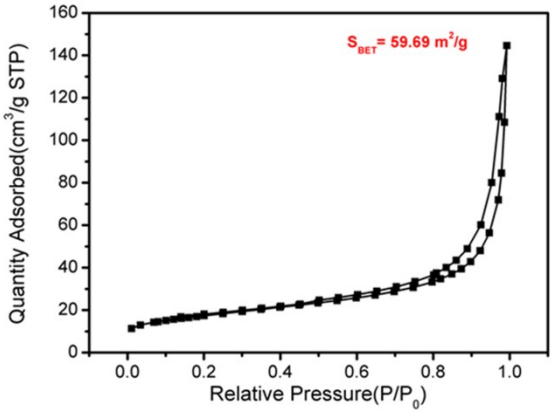

Figure S4 N_2 adsorption-desorption isotherms of g-C_3N_4

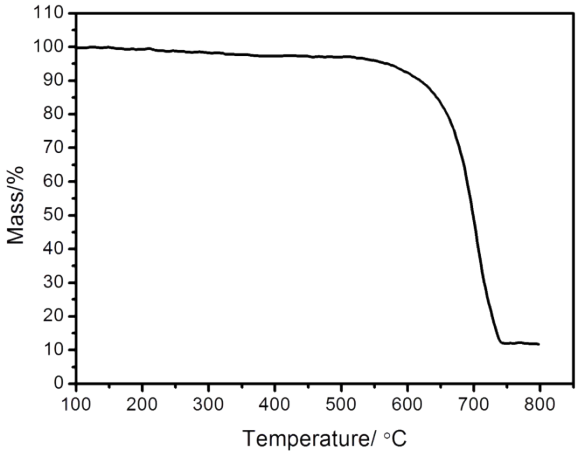

Figure S5 The TGA of g-C_3N_4

The TGA result is shown in Figure S5. The beginning temperature of the weight loss is approximately at 600 °C, indicating the g-C_3N_4 has good thermal stability.

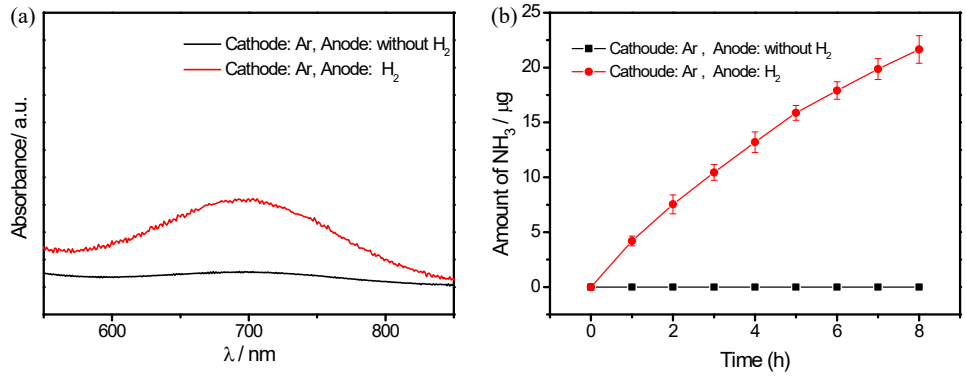

Figure S6 (a) UV-vis absorption spectra of the cathodic absorption with indophenol indicator obtained after electrochemical reaction for 2 hours when only fed by Ar in the cathode chamber (applied potential –1.0 V vs RHE), (b) the amount of NH_3 in cathodic absorption over time when the cathode is supplied with Ar.

In this work, the applied potential is -1.0 V vs RHE. The anode cannot provide H^+ when no H_2 fed in the anode chamber, because the H_2O cannot be electrolyzed to produce H^+ under this applied potential. No ammonia was detected when only fed by Ar in the cathode and no H_2 fed in the anode chamber under -1.0 V vs RHE, suggesting that there are no NH_3 adsorbed on the catalyst surface. But when simultaneously fed Ar in the cathode and H_2 in the anode chamber, the absorbance of the cathodic absorption with indophenol indicator is relatively

higher than that without H_2 in the anode, indicating the NH_3 is formed in the cathode. And the NH_3 is formed by the surface N in g-C_3N_4 and the H^+ from the anode.

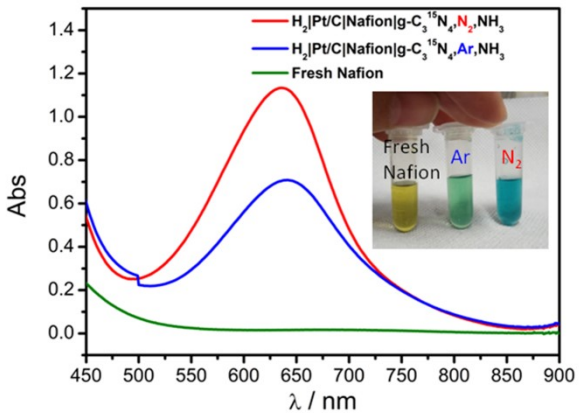

Figure S7 UV−vis absorption spectra of the ammonia in the soaking solution of the used Nafion 212 membrane obtained after electrochemical reaction for 8 hours when the cathode fed by Ar or N_2 followed by the indophenol assay. The inset photos show the color change of the solutions by the indophenol assay.

After using the g-$C_3{}^{15}N_4$ as catalyst for ENRR, the obtained soaking solutions of the used Nafion 212 were treated with phenol in the presence of NaClO as oxidizing reagent and $Na_2[Fe(CN)_5NO]$ as catalyst. As is shown in Figure S8, both solutions show distinctive absorption at 630 nm assigned to indophenol. When fed by Ar or N_2 in the cathode chamber, NH_3 can be detected in the used Nafion 212 after electrochemical reaction for 8 hours. And the absorbance of the soaking solution with indophenol indicator when the cathode fed by N_2 is relatively higher than that of fed by Ar, indicating that g-C_3N_4 not only acts as the nitrogen source but also acts as an electrocatalyst for the nitrogen reduction reaction. In addition, no ammonia was detected in the fresh Nafion 212.

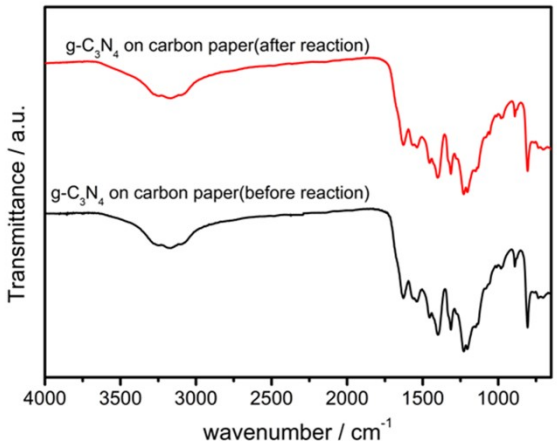

Figure S8 FT-IR spectra of the catalyst g-C_3N_4 before/after the reaction.

As observed in Figure S8, there is no notable difference in FT-IR spectra of the g-C_3N_4 after reaction, suggesting its good chemical stability.

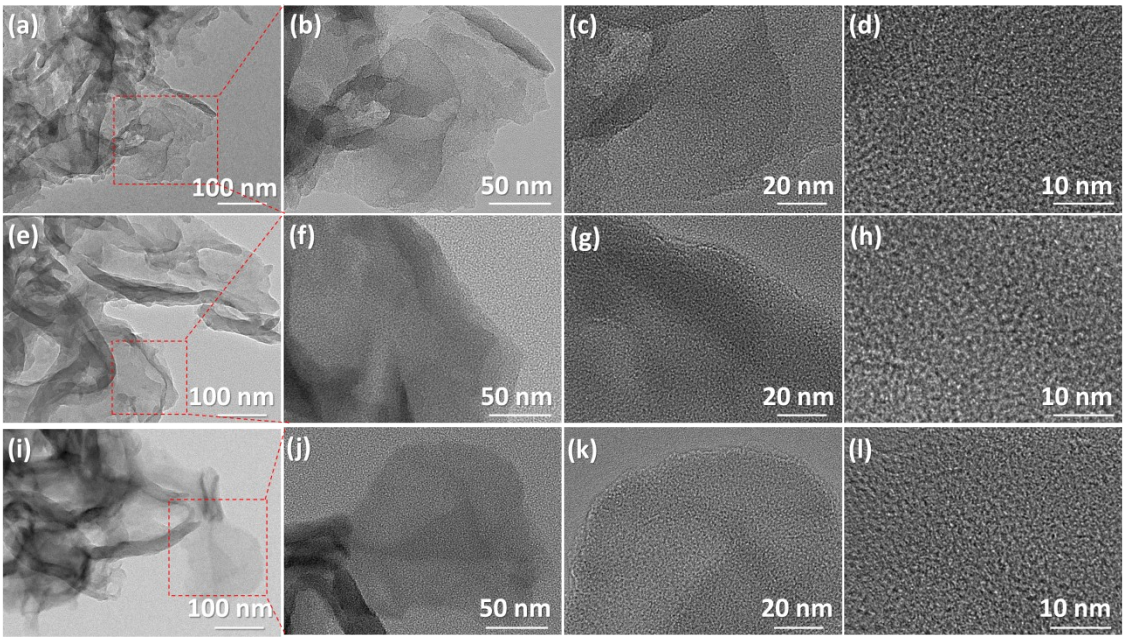

Fig. S9 TEM images of the fresh g-C3N4 (a-d), the used g-C_3N_4 in Ar after ENRR (e-h), and the used g-C_3N_4 in N_2 after ENRR (i-l).

The high magnification TEM images of the fresh and used g-C_3N_4 in Ar and N_2 are presented in Fig. S9 From the TEM images, no significant morphological changes are observed in the fresh and used samples after ENRR in Ar and N_2.

Fig. S10 Schematic of the designed electrochemical cell for ATR-FTIR

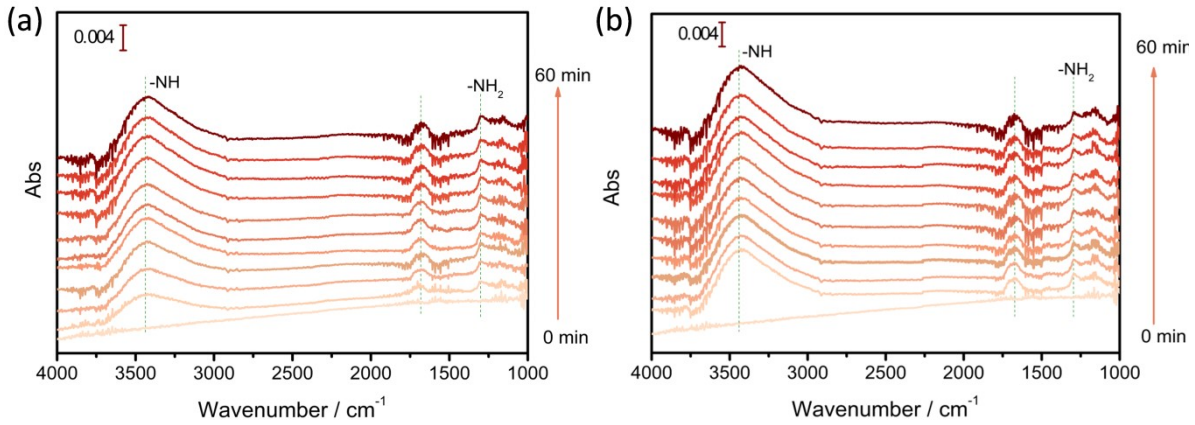

Fig. S11 *In situ* FTIR spectra obtained on the surface of g-$C_3{}^{15}N_4$ (-1.0 V vs RHE) for (a) Ar and (b) N_2 bubbled 0.005 M H_2SO_4 aqueous solution. The background for the system has been subtracted from the spectra.

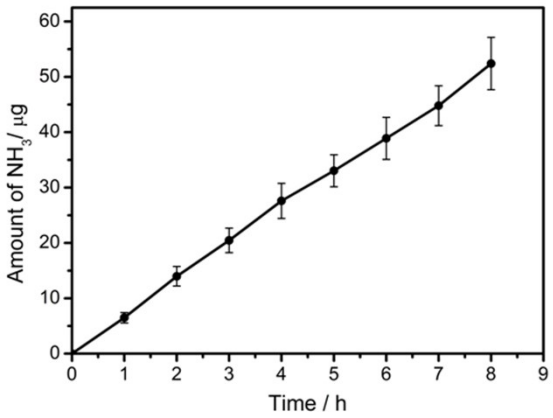

Figure S12 The amount of ammonia in the cathodic absorption solution over time under the catalyst g-C_3N_4 when the cathode is supplied with N_2.

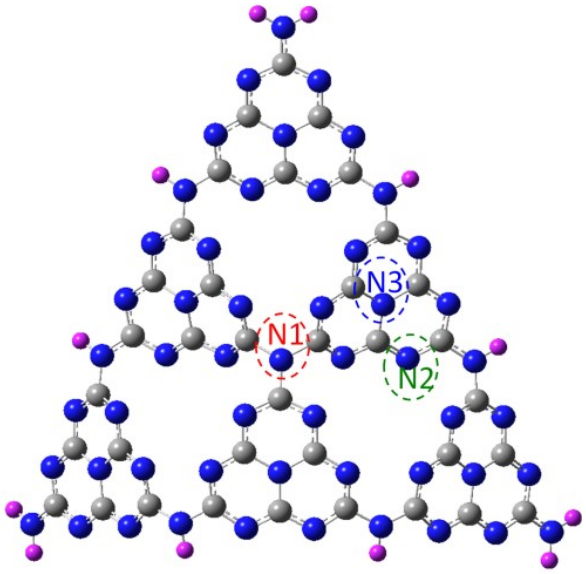

Figure S13 The optimized structure of g-C_3N_4 monolayer. The gray, blue ,and purples spheres represent the carbon, nitrogen ,and hydrogen atoms, respectively, and different nitrogen sites are labeled.

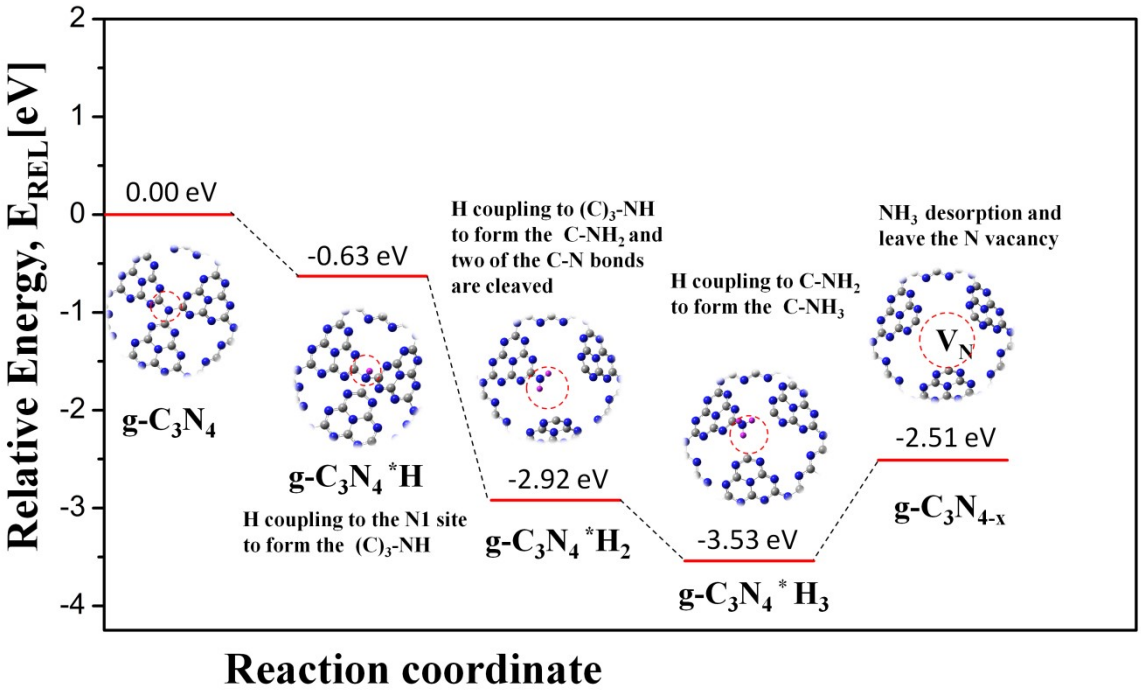

Figure S14 The formation of NH_3 via abstraction of g-C_3N_4 surface nitrogen atom by protonation on N1 site and leave behind N vacancy.

A proton absorbs on the N1 site in the catalyst g-C_3N_4 and forms $(C)_3$–NH (g-C_3N_4*H), which releases 0.63 eV. Then the second H atom was absorbed on the N1 site to form C–NH_2 with releasing 2.29 eV and two of the C–N bonds between the N1 site with the C of tri-s-triazine were cleaved. This step is followed by adding the third proton on C-NH_2 to generated the C–NH_3, an exothermic step that which releases around 0.61 eV. The last step is the desorption of the NH_3 molecule, which is an endothermic process (barrier of 1.02 eV), and then leaves behind an N vacancy.

20

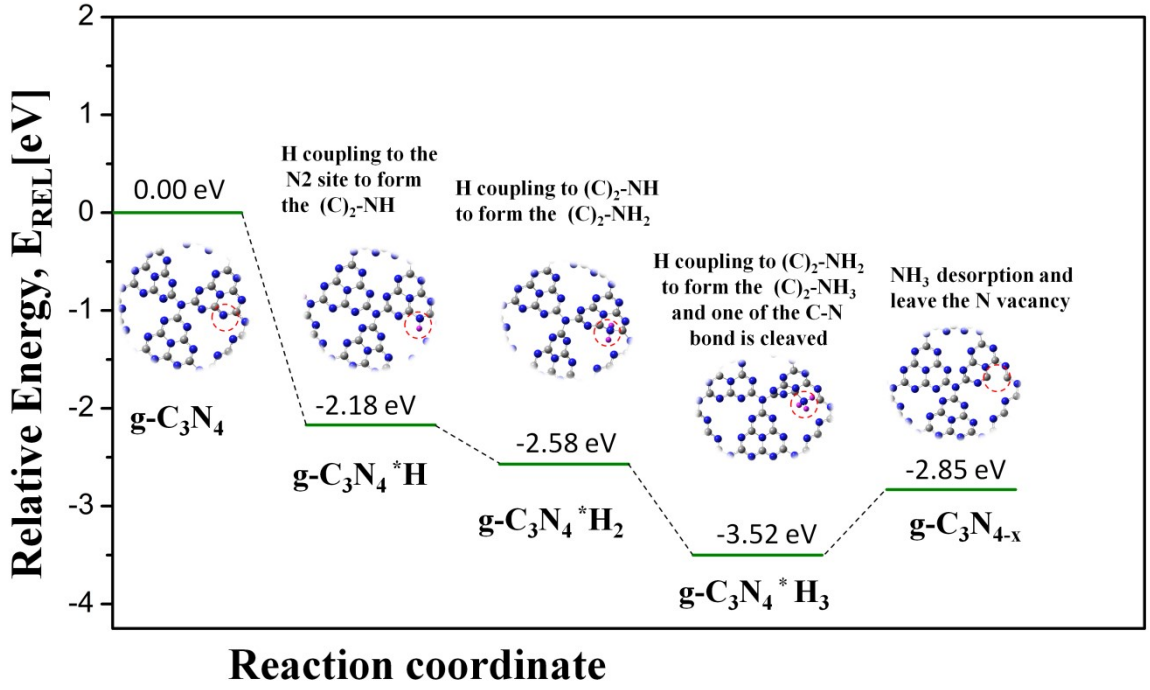

Figure S15 The formation of NH_3 via abstraction of g-C_3N_4 surface nitrogen atom by protonation on N2 site and leave behind N vacancy.

As shown in Figure S12, the first H atom coupling to the N2 site in g-C_3N_4 to form $(C)_2$–NH is a spontaneous process with releasing 2.18 eV. This step is followed by spontaneously reacting with another H to form $(C)_2$–NH_2 (ΔG= –0.40 eV). Then, the third H coupling to $(C)_2$–NH_2 to form C-NH_3, and one of the C-N bonds between the N2 site and the adjacent C atoms is cleaved. The detachment of NH_3 requires 0.67 eV and then leaves behind the N vacancy in the N2 site.

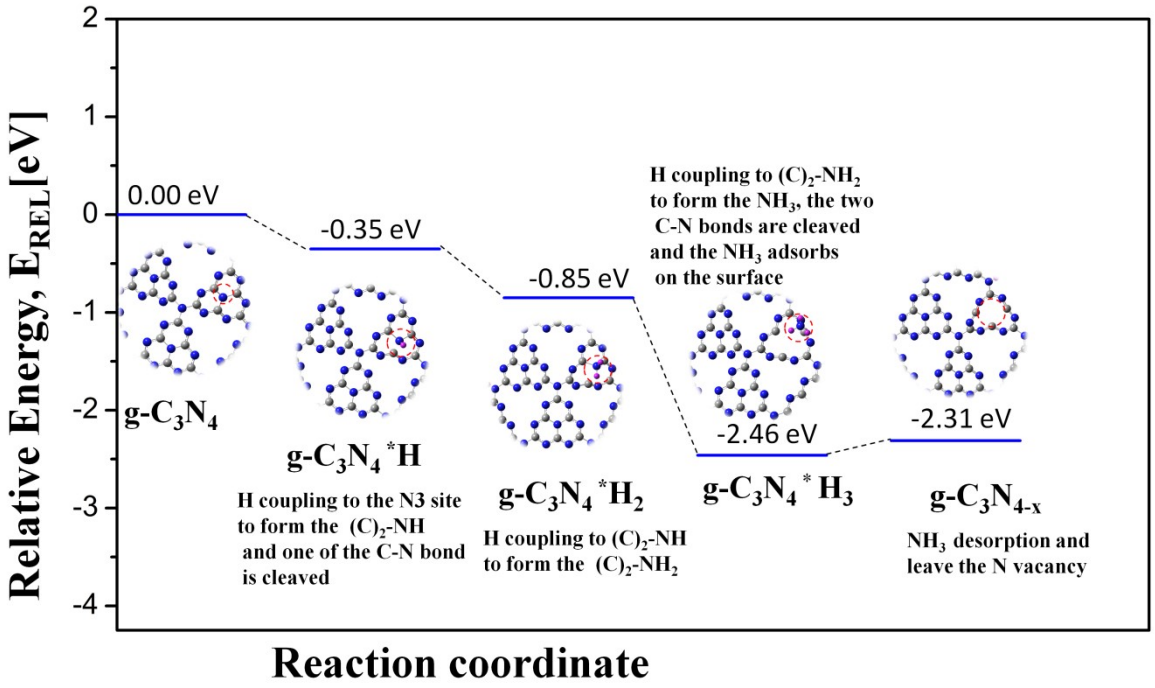

Figure S16 The formation of NH_3 via abstraction of g-C_3N_4 surface nitrogen atom by protonation on N3 site and leave behind N vacancy.

The N3 site also can generate NH_3 by hydrogenation process and the detailed steps are shown in Figure S13. The first H coupling to the N3 site to form $(C)_2$–NH and one of the C–N bonds between the N3 site and neighboring C atoms is cleaved with releasing 0.35 eV. Then two consecutive H couplings to $(C)_2$–NH to form $(C)_2$–NH_2 and NH_3 also are barrierless. And the detachment of NH_3 requires 0.15 eV.

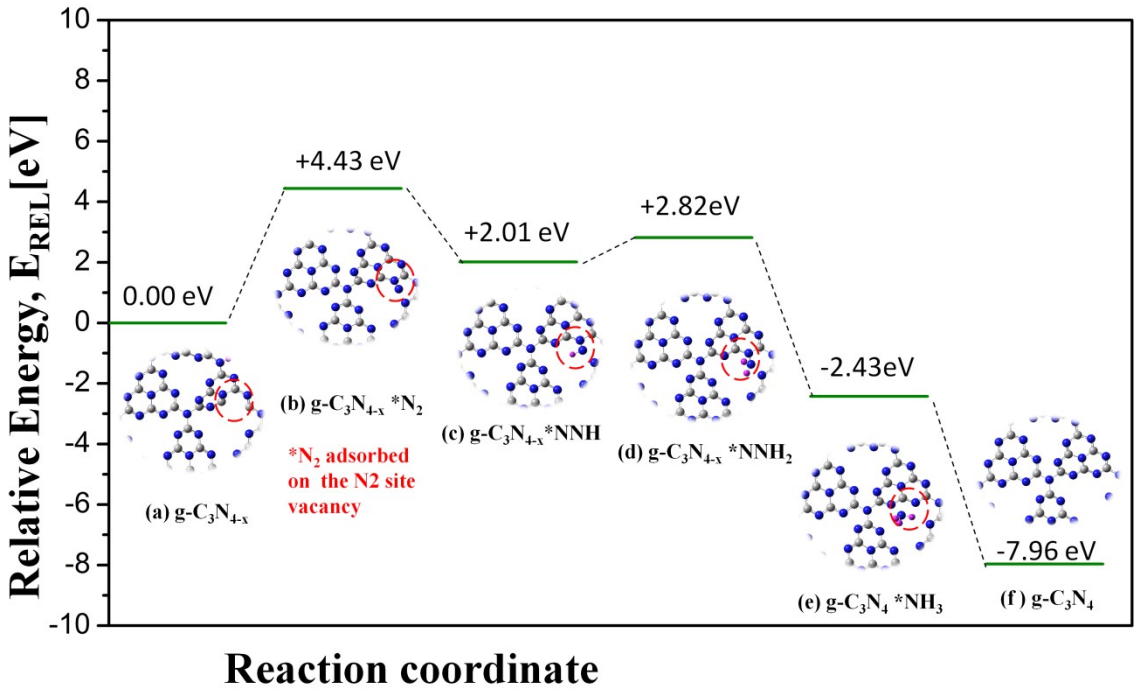

Figure S17 The refilling process of an N vacancy (N2 site) on g-C_3N_4 and in the activation of N_2 molecule on N vacancy. Relative energies are given to the reactants g-C_3N_{4-x}

The insertion of N_2 into the N2 site vacancy is endothermic, with an adsorption energy of 4.43 eV. After that, the H atoms were adsorbed on the activated N_2 molecule, and then the N-H bonds are formed. The first H coupling to the adsorbed $^*N_2$ to $^*N_2H$ is barrierless ($\Delta G = -2.42$ eV). The second H coupling to $^*N_2H$ to form $^*N_2H_2$ requires 0.81 eV. This step is followed by adding the third proton on $^*N_2H_2$ generated the $^*N_2H_3$, an exothermic step that which releases around 5.25 eV. The last step is the desorption of the NH_3 molecule ($\Delta G = -5.53$ eV).

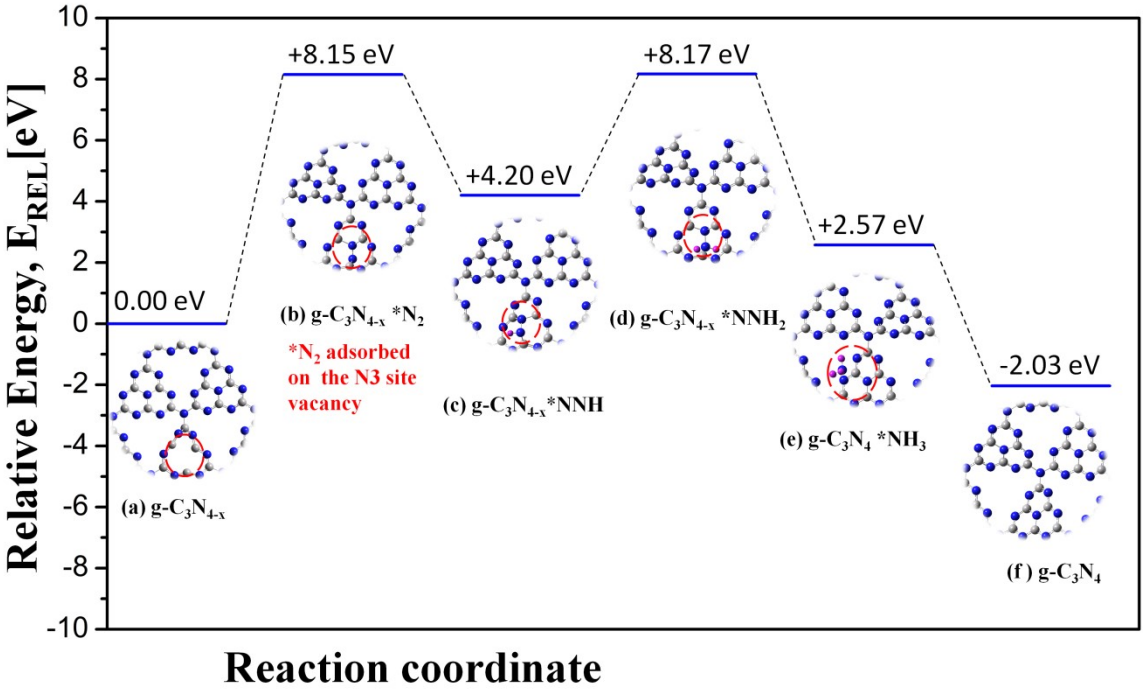

Figure S18 The refilling process of an N vacancy (N2 site) on g-C_3N_4 and in the activation of N_2 molecule on N vacancy. Relative energies are given to the reactants g-C_3N_{4-x}

The process of N vacancy refiliing on N3 site was also simulated computationally. The energetics of teh catalyst regenerated process and the second NH3 formation process are illustrated in Figure S18. We begin with teh adsorption of molecule nitrogen close teh N3 vacancy, which is endothermic with the N2 molecule adsorption energy of around 8.15 eV. After the N_2 molecule adsorbed on teh N3 site vacancy, teh H atoms were adsorbed on teh activated N2 molecule, and then teh N-H bonds are formed (Figure S18c-e). It can be found that the first H coupling to the adsorbed $^*N_2$ to $^*N_2H$ is barrierless ($\Delta G = -3.95$ eV). The second H coupling to $^*N_2H$ to form $^*N_2H_2$ requires 3.97 eV. This step is followed by adding the third proton on $^*N_2H_2$ generated the $^*N_2H_3$, an exothermic step that which releases around 5.60 eV. The last step is the desorption of the NH_3 molecule ($\Delta G = -4.60$ eV). The complete catalyic cycle involving surface N abstraction by protons and N vacancy refilling on N3 site is summarized in Figure S20.

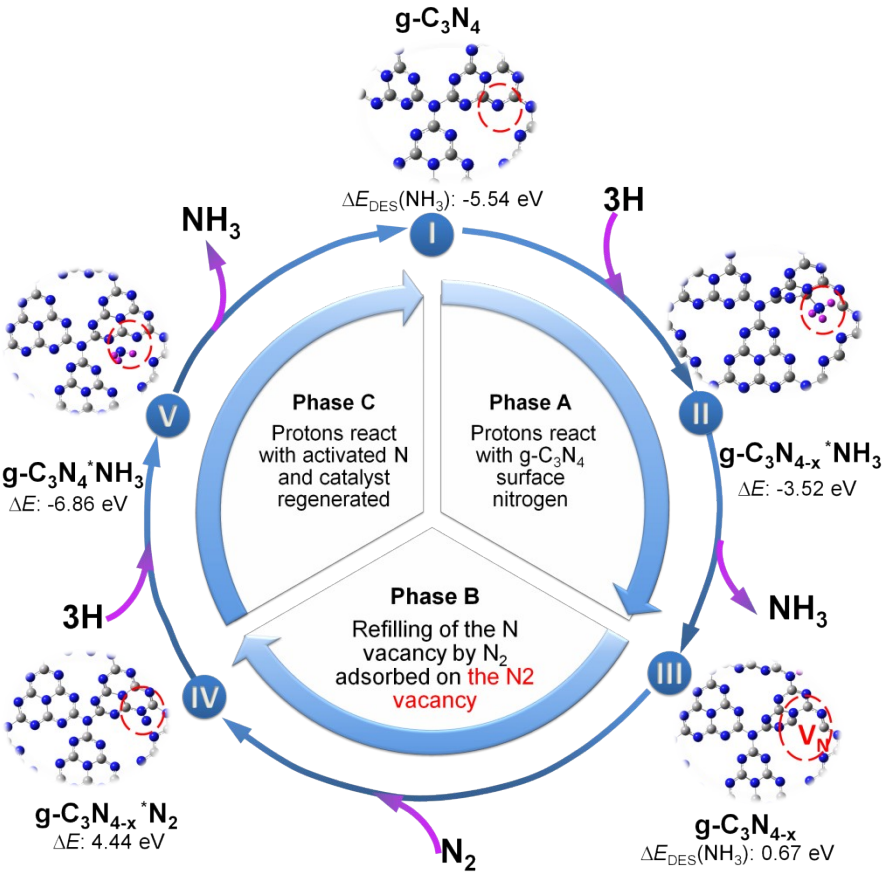

Figure S19 Proposed catalytic cycle for N_2 reduction on g-C_3N_4(N2 site). In phase A, a surface N atom in the catalyst is abstracted by H to form NH_3 and an N vacancy. In phase B, the N_2 molecule is bridged in the N vacancy of N1 site. In phase C, the bridged N_2 is activated by H, under the formation of the second NH_3 molecule and the catalyst is regenerated.

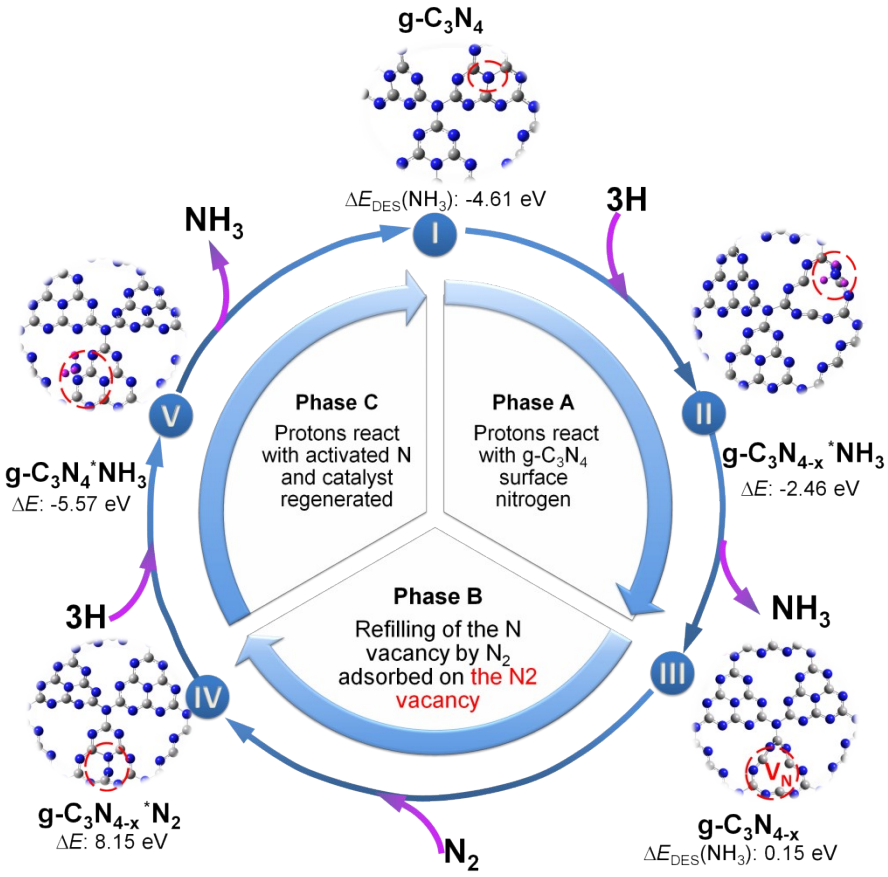

Figure S20 Proposed catalytic cycle for N_2 reduction on g-C_3N_4(N3 site). In phase A, a surface N atom in the catalyst is abstracted by H to form NH_3 and an N vacancy. In phase B, the N_2 molecule is bridged in the N vacancy of N1 site. In phase C, the bridged N_2 is activated by H, under the formation of the second NH_3 molecule and the catalyst is regenerated.

Tables:

Table S1 The amount of ammonia, the ammonia production rate, and the Faradaic efficiency over the catalyst g-C_3N_4 for nitrogen reduction at -1.0 V vs RHE for 8 h (repeated experiment)

Cell	M_c/μg	M_a/μg	M_m/μg	M_t/μg	R/(mol $cm^{-2}s^{-1}$)	R_{ave}/(mol $cm^{-2}s^{-1}$)	FE/ %	FE_{ave}/ %
H_2,Pt/C|Nafion|g-C_3N_4,N_2,NH_3	57.65	6.38	274.39	338.42	1.75×10^{-10}		1.57	
H_2,Pt/C|Nafion|g-C_3N_4, N_2,NH_3	46.55	5.30	269.91	321.76	1.66×10^{-10}	1.62×10^{-10}	1.34	1.39
H_2,Pt/C|Nafion|g-C_3N_4,N_2,NH_3	51.01	4.11	224.99	280.11	1.44×10^{-10}		1.26	

Note: M_c is the amount of ammonia in the cathodic absorption，M_a is the amount of ammonia in the anode absorption, M_m is the amount of ammonia in the soaking solution of the used Nafion 212 membrane obtained after electrochemical reaction, M_t is the total of ammonia.

Table S2 The amount of ammonia over the catalyst g-$C_3{}^{15}N_4$ when the cathode is supplied with N_2/Ar at -1.0 V vs RHE for 8 h

Cell	M_c/μg	M_a/μg	M_m/μg	M_t/μg
H_2,Pt/C|Nafion|g-$C_3{}^{15}N_4$,N_2,NH_3	59.69	6.97	285.39	352.05
H_2,Pt/C|Nafion|g-$C_3{}^{15}N_4$,Ar,NH_3	21.65	3.30	132.96	157.91

During the ENRR, most of the produced NH_3 was trapped in the Nafion membrane, because of the strong interactions between NH_3 and Nafion membrane. In the 0.005M H_2SO_4 absorption solution, the produced NH_3 could be predominantly detected in the cathode exhausts, which is expected as NH_3 is only produced at the cathode. When the cathode is supplied with N_2, the amount of ammonia in the cathodic absorption and the used Nafion 212 membrane is higher than that of the cathode is supplied with Ar, suggesting that the catalyst g-C_3N_4 can electro-catalyze N_2 to NH_3.

XPS results

Table S3 Surface elemental contents of fresh and used g-C_3N_4 catalysts without 5 wt% Nafion

Samples	Element content (at%)			C/N atomic ratio
	C	N	O	
Fresh g-C_3N_4	46.09	**52.12**	1.79	0.884
Used g-C_3N_4(Ar)	46.36	**50.67**	2.97	0.915
Used g-C_3N_4(N_2)	46.26	**51.34**	2.40	0.901

Note: To rule out the influence of carbon paper and the Nafion on catalyst g-C_3N_4 composition, the catalysts g-C_3N_4 were dispersed in 0.005 M H_2SO_4 aqueous solution, and Pt foil was used as the work electrode with Ar/N_2 at -0.1 V vs RHE. The samples for XPS analysis were without 5 wt% Nafion solution.

Table S4 N species content (at%) of fresh and used g-C_3N_4 catalysts

Sample	C=N-C (N2 site)	N-$(C)_3$ (N1site and N3site)	C-NH
Fresh g-C_3N_4	47.07%	**30.21%**	22.72%
Used g-C_3N_4(Ar)	50.35%	**28.94%**	20.71%
Used g-C_3N_4(N_2)	48.08%	**29.53%**	22.39%

EA results

Table S5 The Elementar analysis of the fresh and used g-C_3N_4 catalysts without 5 wt% Nafion solution.

Samples	Element content (wt%)				C/N
	C	N	H	O	atomic ratio
Fresh g-C_3N_4	33.535±0.025	**61.415±0.055**	2.310±0.010	2.740±0.020	0.637
Used g-C_3N_4(Ar)	33.370±0.060	**59.935±0.025**	2.430±0.010	4.265±0.045	0.649
Used g-C_3N_4(N_2)	33.215±0.005	**60.160±0.050**	2.385±0.005	4.240±0.050	0.645

Note: The samples for elemental analysis were without 5 wt% Nafion solution.

To further rule out the influence of Nafion on catalyst g-C_3N_4 composition, the catalysts g-C_3N_4 were dispersed in 0.005 M H_2SO_4 aqueous solution, and Pt foil was used as the work electrode with Ar/N_2 at -0.1 V vs RHE. And then we used elemental analysis to determine the content of C, N, and H in the fresh/used g-C_3N_4. Since Nafion solution was not added, and combine with XPS data, so that g-C_3N_4 contained four elements C, H, N, and O. After the element contents of C, H, and N were determined, the remaining was considered as O. As listed in Table S5, the atomic ratios of carbon to nitrogen in the samples are 0.63 ~ 0.65, lower than 0.75 for the ideal g-C_3N_4, and the hydrogen and oxygen elements detected are indicative of the incomplete thermal condensation of urea. The content of C element is almost unchanged before and after the reaction (Table S5). The contents of N and O elements vary before and after the reaction. Before the reaction, the content of N in the fresh g-C_3N_4 is 61.415 ± 0.055 wt%. When fed by Ar in the cathode, the content of N in the used g-C_3N_4 decreased from 61.415 ± 0.055wt% to 59.935 ± 0.025 wt%. These results reveal that the surface N atoms in g-C_3N_4 might be used to produce NH_3, and the N vacancies are created. Compared with the Ar atmosphere, the content of N in the used g-C_3N_4 has a slight increase (from 59.935± 0.025 wt% to 60.160 ± 0.050 wt%) when fed by N_2 in solution, suggesting the N vacancies could be replenished with N_2 molecules. But the content of N in the used g-C_3N_4

under N_2 supplying is slightly lower than that of fresh g-C_3N_4, indicating that the N vacancies might not be completely refilled with the N_2. That could explain why the rate of producing NH_3 in the second cycle of the alternating test by fed Ar is slower than that of the first cycle. In addition, after the reaction, the content of the O element was higher than that in the fresh catalyst, which was also consistent with the XPS data.

References:

1. C. Li, T. Wang, Z. J. Zhao, W. Yang, J. F. Li, A. Li, Z. Yang, G. A. Ozin and J. Gong, *Angewandte Chemie*, 2018, **57**, 5278-5282.
2. C. Lv, Y. Qian, C. Yan, Y. Ding, Y. Liu, G. Chen and G. Yu, *Angewandte Chemie*, 2018, **57**, 10246-10250.
3. A. Banerjee, B. D. Yuhas, E. A. Margulies, Y. Zhang, Y. Shim, M. R. Wasielewski and M. G. Kanatzidis, *Journal of the American Chemical Society*, 2015, **137**, 2030-2034.
4. W. J. Ong, L. L. Tan, Y. H. Ng, S. T. Yong and S. P. Chai, *Chemical reviews*, 2016, **116**, 7159-7329.
5. J. R. C. G. M. A. R. G. W. T. H. M. J. Frisch, H. N. M. C. G. A. Petersson, J. B. G. Z. A. F. Izmaylov, K. T. R. F. M. Ehara, Jr. O. K. H. N. Y. Honda, F. O. M. B. J. E. Peralta, V. N. S. T. K. N. Kudin, A. R. J. C. K. Raghavachari, N. R. J. M. M. Cossi, C.A. J. J. V. Bakken, A. J. A. R. O. Yazyev, K. M. V. G. R. L. Martin, J. J. D. S. P. Salvador, J. B. F. J. O. Farkas and D. J. Fox, Gaussian, Inc., Wallingford CT, 2010.
6. A. D. Becke, *J Chem Phys*, 1993, **98**, 5648-5652.
7. A. B. G. A. Petersson, Thomas G. Tensfeldt, Mohammad A. AI-Laham, and and W. A. Shirley, *J Chem Phys*, 1988, **89**, 2193-2218.
8. G. A. P. a. M. A. AI-Laham, *J Chem Phys*, 1991, **94**, 6081-6090.
9. S. Grimme, S. Ehrlich and L. Goerigk, *J Comput Chem*, 2011, **32**, 1456-1465.
10. E. Caldeweyher, C. Bannwarth and S. Grimme, *J Chem Phys*, 2017, **147**, 034112.